Efficient and easily repeatable organic solar cells under high boiling point solvent by introducing highly mixed tolerant guest acceptor

Xiangyu Shen,‡[a,b] Xiaoning Wang,‡[b,c,d] Jianxiao Wang,*[b,c,d] Rulin Wang,*[a] Yonghai Li,[b,c,d] Fuzhen Bi,*[b,c,d] Xichang Bao[b,c,d]

[a] Centre for Theoretical and Computational Physics, College of Physics, Qingdao University, Qingdao 266071, China

[b] Key Laboratory of Photoelectric Conversion and Utilization of Solar Energy, Qingdao Institute of Bioenergy and Bioprocess Technology, Chinese Academy of Sciences

Qingdao 266101, China

[c] Functional Laboratory of Solar Energy, Shandong Energy Institute, Qingdao 266101, China

[d] Qingdao New Energy Shandong Laboratory, Qingdao 266101, China

* Corresponding author

E-mail addresses: wangjianxiao@qibebt.ac.cn; rulin11@qdu.edu.cn; bifz@qibebt.ac.cn

1. The synthesis details for the acceptor L8BO-2O

Synthesis of 4,7-dibromo-2-(2-(2-methoxyethoxy)ethyl)-2H-benzo[d][1,2,3]triazole(2)

4,7-dibromo-2H-benzo[d][1,2,3]triazole (1.11 g, 4 mmol), 1-bromo-2-(2-methoxyethoxy)ethane (1.10 g, 6 mmol) and powdered K_2CO_3 (1.38 g, 10 mmol) were dissolved in DMF(10 mL) and stirred at 100 °C overnight under nitrogen. The reaction mixture was allowed to cool to room temperature and spin dry with dichloromethane and water. Further purification by column chromatography using ethyl acetate/petroleum ether (1/2.5, v/v) as eluent to afford colorless oil compound 2 with a yield of 47% (0.54 g). ^{1}H NMR (600 MHz, $CDCl_3$) δ 7.44 (s, 2H), 4.97 (t, 2H), 4.21 (t, 2H), 3.64 (m, 2H), 3.48 (m, 2H), 3.32 (s, 3H).

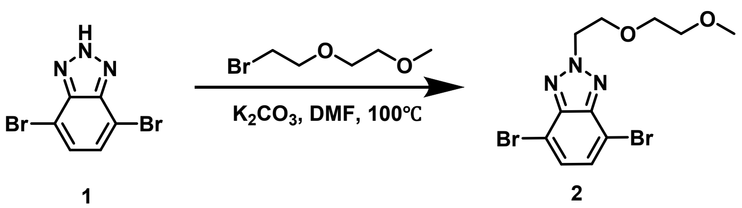

Figure S1 Synthetic route of 4,7-dibromo-2-(2-(2-methoxyethoxy)ethyl)-2H-benzo[d][1,2,3]triazole.

Synthesis of 4,7-dibromo-2-(2-(2-methoxyethoxy)ethyl)-5,6-dinitro-2H-benzo[d][1,2,3]triazole(3)

Add concentrated sulfuric acid (5 mL) and Compound 2 to 50 mL flask and stirred at 0 °C. After 30 min, slowly add fuming nitric acid and then continue stirring for 4 h. The reaction mixture was poured into ice water (50 mL) and then extracted with dichloromethane and brine. It was steamed under reduced pressure and dried over $NaSO_4$. The crude product was purified on silica gel chromatography using petroleum ether/ ethyl acetate (1:1, v/v) to give compound 3 (0.56 g) as a yellow solid in a yield of 90%.

^{1}H NMR (600 MHz, $CDCl_3$) δ 5.04 (t, J = 5.4 Hz, 2H), 4.24 (t, J = 5.4 Hz, 2H), 3.71 – 3.59 (m, 2H), 3.54 – 3.42 (m, 2H), 3.33 (s, 3H).

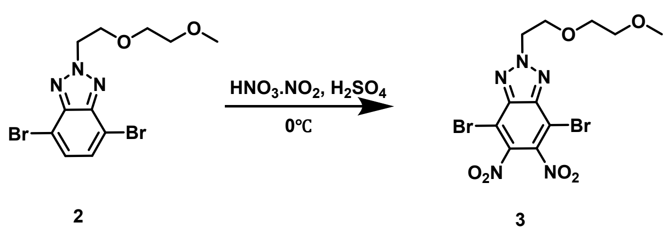

Figure S2 Synthetic route of 4,7-dibromo-2-(2-(2-methoxyethoxy)ethyl)-5,6-dinitro-2Hbenzo[d][1,2,3]triazole.

Synthesis of 4,7-bis(6-(2-butyloctyl)thieno[3,2-b]thiophen-2-yl)-2-(2-(2-methoxyethoxy)ethyl)-5,6-dinitro-2H-benzo[d][1,2,3]triazole(5)

Tributyl(6-(2-butyloctyl)thieno[3,2-b]thiophen-2-yl)stannane (2.34 g, 3.916 mmol), compound 3 (0.57 g, 1.215 mmol) and $Pd(PPh_3)Cl_2$ (0.62 g,0.88 mmol) were dissolved in 25 mL of dry toluene and stirred at 100 °C overnight. The reaction mixture was allowed to cool to room temperature and then concentrated under reduced pressure. The crude product was chromatographically purified on a silica gel column eluting with petroleum ether /dichloromethane (1/2, v/v) as the eluent to afford compound 5 as a red solid (1.11 g, 99% yield).

^{1}H NMR (600 MHz, $CDCl_3$) δ 7.77 (s, 1H), 7.12 (s, 2H), 5.02 (t, J = 5.5 Hz, 2H), 4.22 (t, J = 5.6 Hz, 2H), 3.63 (m, J = 5.4, 3.7 Hz, 2H), 3.48 (m, J = 5.4, 3.7 Hz, 2H), 3.31 (s, 3H), 2.70 (d, J = 7.0 Hz,4H), 1.68 – 1.59 (m, 2H), 1.42 – 1.17 (m, 36H), 0.96 – 0.81 (m, 12H).

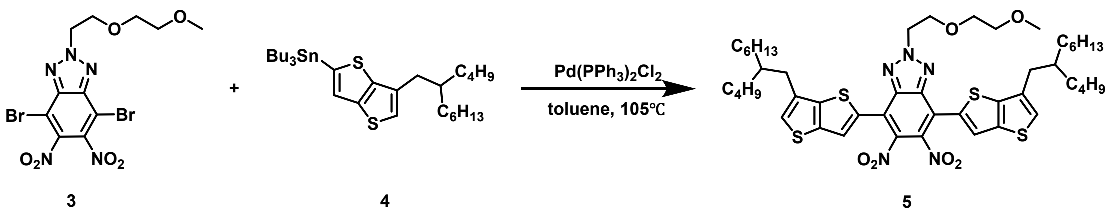

Figure S3 Synthesis route of 4,7-bis(6-(2-butyloctyl)thieno[3,2-b]thiophen-2-yl)-2-(2-(2-methoxyethoxy)ethyl)-5,6-dinitro-2H-benzo[d][1,2,3]triazole.

Synthesis of 3,9-bis(2-butyloctyl)-12,13-bis(2-ethylhexyl)-6-(2-(2-methoxy-ethoxy)ethyl)-12,13-dihydro-6H-thieno[2'',3'':4',5']thieno[2',3':4,5]pyrrolo[3,2-g]thieno[2',3':4,5]thieno[3,2-b][1,2,3]triazolo[4,5-e]indole(6)

Compound 5 (1.0 g, 1.08 mmol) and triphenyl phosphorus (2.84 g, 10.8 mmol) were dissolved in the o-dichlorobenzene (o-DCB, 20 mL) under nitrogen. After being heated at 180 °C overnight, the aqueous phase was extracted with dichloromethane and the organic layer was dried over Na_2SO_4 and filtered. After removing the solvent, the brown residue was chromatographically purified on a silica gel column eluting to remove most of the impurities, such as the remaining triphenyl phosphorus and by-product triphenyl phosphorus oxide. The purified brown solid (0.5g), K_2CO_3 (0.4 g, 2.9 mmol), 1-Bromo-2-ethylhexane (0.448 g, 2.32 mmol) and DMF (20 mL) were taken in a two-neck flask, and stirred at 80 °C overnight under nitrogen. Cool to room temperature and spin dry with ethyl acetate and water. Further purification by column chromatography using petroleum ether/dichloromethane (1/3, v/v) as eluent to afford red solid 6 (0.45 g, 35% yield).

^{1}H NMR (600 MHz, $CDCl_3$) δ 6.95 (s, 2H), 5.03 (t, J = 6.2 Hz, 2H), 4.58 (d, J = 7.7 Hz, 4H), 4.29 (t, J = 6.2 Hz, 2H), 3.70 (m, J = 5.5, 3.7 Hz, 2H), 3.54 (m, J = 5.6, 3.7 Hz, 2H), 3.34 (s, 3H), 2.74 (d, J = 7.2 Hz, 4H), 2.03 – 1.94 (m, 4H), 1.44 – 1.23 (m, 50H), 0.98 – 0.78 (m, 36H), 0.67 – 0.48 (m, 12H).

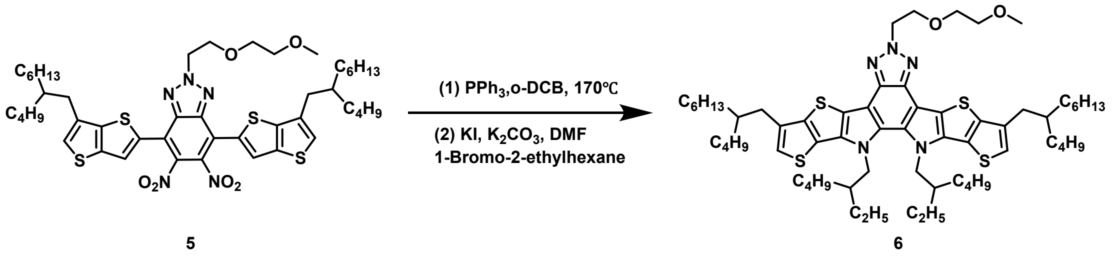

Figure S4 Synthesis route of 3,9-bis(2-butyloctyl)-12,13-bis(2-ethylhexyl)-6-(2-(2-methoxy-ethoxy)ethyl)-12,13-dihydro-6H-thieno[2",3":4',5']thieno[2',3':4,5]pyrrolo[3,2-g]thieno[2',3':4,5]thieno[3,2-b][1,2,3]triazolo[4,5-e]indole.

Synthesis of 3,9-bis(2-butyloctyl)-12,13-bis(2-ethylhexyl)-6-(2-(2-methoxye-thoxy)ethyl)-12,13-dihydro-6H-thieno[2",3":4',5']thieno[2',3':4,5]pyrrolo[3,2-g]thieno[2',3':4,5]thieno[3,2-b][1,2,3]triazolo[4,5-e]indole-2,10-dicarbaldehyde(7)

DMF and 1, 2-Dichloroethane was take into 50 mL two-neck flask and stirred at 0 °C，after 15 min, $POCl_3$ was added and continue stirred at 0 °C for 2 h. 10 mL 1, 2-Dichloroethane with compound 6 (230 mg, 0.21 mmol) was added at 0 °C and heated to 70 °C for 15 h after completion of the addition, the mixture was quenched with saturated CH_3COONa solution and extracted with ethyl acetate. The organic phase was dried over Na_2SO_4 and filtered. After removing the solvent, the residue was purified by column chromatography on silica gel using petroleum ether/dichloromethane (1/6, v/v) as eluent to afford red solid 7 (0.23 g, 95% yield).

^{1}H NMR (600 MHz, $CDCl_3$) δ 10.11 (s, 2H), 5.04 (t, J = 6.0 Hz, 2H), 4.63 – 4.59 (m, 2H), 4.30 (t, J = 6.0 Hz, 2H), 3.71 (m, J = 6.3, 2.8 Hz, 2H), 3.57 – 3.52 (m, 2H), 3.34 (s, 3H), 3.10 (d, J = 7.5 Hz,4H), 2.11 – 2.03 (m, 2H), 2.01 – 1.87 (m, 2H), 1.46 – 1.22 (m, 32H), 1.04 – 0.75 (m, 26H), 0.68 – 0.60 (m, 6H), 0.56 (m, J = 14.3, 7.2 Hz, 6H).

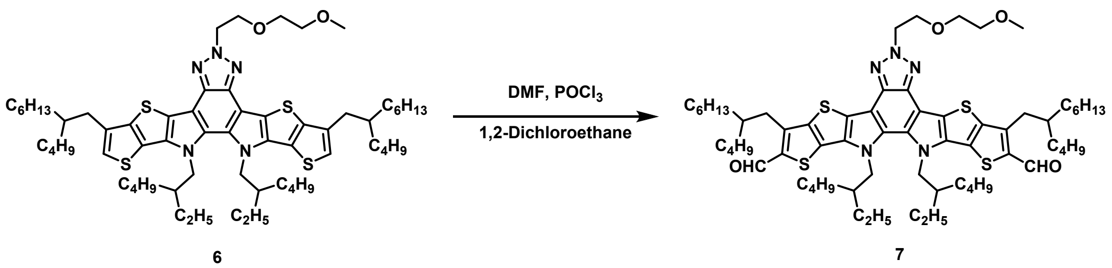

Figure S5 Synthesis route of 3,9-bis(2-butyloctyl)-12,13-bis(2-ethylhexyl)-6-(2-(2-methoxyethoxy)ethyl)-12,13-dihydro-6H-thieno[2'',3'':4',5']thieno[2',3':4,5]pyrrolo[3,2-g]thieno[2',3':4,5]thieno[3,2-b][1,2,3]triazolo[4,5-e]indole-2,10-dicarbaldehyde.

Synthesis of 2,2'-((2Z,2'Z)-((3,9-bis(2-butyloctyl)-12,13-bis(2-ethylhexyl)-6-(2-(2-methoxyethoxy)ethyl)-12,13-dihydro-6H-thieno[2'',3'':4',5']thieno[2',3':4,5] pyrrolo[3,2-g]thieno[2',3':4,5]thieno[3,2-b][1,2,3]triazolo[4,5-e]indole-2,10-diyl)bis(methaneylylidene))bis(5,6-difluoro-3-oxo-2,3-dihydro-1H-indene-2,1-diylidene))dimalononitrile(L8BO-2O)

INCN-F (46 mg, 0.202 mmol) and compound 7 (100 mg, 0.088 mmol) were added to a solvent mixture of chloroform (15 mL) and pyridine (1 ml). The reaction was placed in an oil bath at 65°C and was stirred for overnight. Removed solvent by reduced pressure and the residue was purified on a silica-gel column chromatography using dichloromethane as eluent to to afford blue solid L8BO-2O (0.96 g, 70% yield).

^{1}H NMR (600 MHz, $CDCl_3$) δ 9.16 (s,2H), 8.59 (m, J = 9.7, 6.5 Hz, 2H), 7.73 (t, J = 7.4 Hz, 2H), 5.08 (t, J = 6.0 Hz, 2H), 4.82 – 4.73 (m, 4H), 4.34 (t, J = 6.0 Hz, 2H), 3.76 (m, J = 5.4, 3.8 Hz, 2H), 3.61 – 3.57 (m, 2H), 3.38 (s, 3H), 3.21 (d, J = 7.6 Hz, 4H), 2.22 – 1.76 (m, 4H), 1.53 – 1.10 (m, 48H), 1.06 – 0.82 (m, 28H), 0.80 – 0.71 (m, 6H), 0.65 (m, J = 7.2, 3.2 Hz, 6H). ^{13}C NMR (151 MHz, $CDCl_3$) δ 186.08, 159.24, 153.64, 145.22, 137.87, 136.32, 135.69, 134.05, 133.56, 129.83, 119.68, 115.30, 114.76, 112.38, 111.86, 71.96, 70.60, 69.53, 68.26, 59.12, 55.74, 55.48, 40.37, 40.13, 34.84, 33.65, 33.39, 31.88, 29.75, 29.67, 28.90, 27.61, 26.64, 23.30, 23.05, 22.80, 22.69, 14.14, 14.12, 13.76, 10.28.

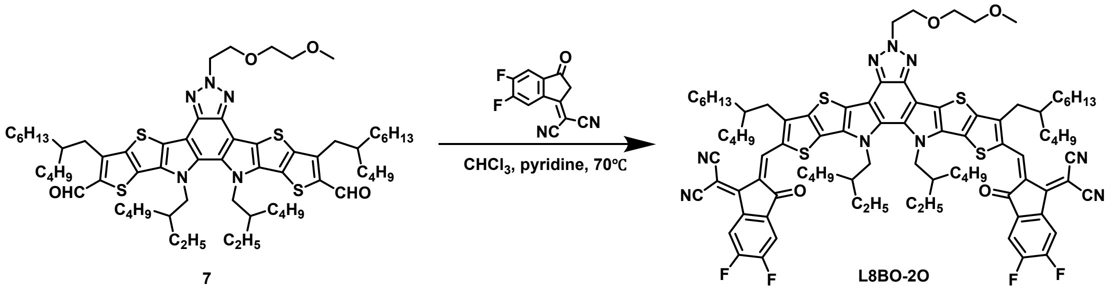

Figure S6 Synthesis route of 2,2'-((2Z,2'Z)-((3,9-bis(2-butyloctyl)-12,13-bis(2-ethylhexyl)-6-(2-(2-methoxyethoxy)ethyl)-12,13-dihydro-6H-thieno[2'',3'':4',5']thieno[2',3':4,5] pyrrolo[3,2-g]thieno[2',3':4,5]thieno[3,2-b][1,2,3]triazolo[4,5-e]indole-2,10-diyl)bis(methaneylylidene))bis(5,6-difluoro-3-oxo-2,3-dihydro-1H-indene-2,1-diylidene))dimalononitrile(L8BO-2O).

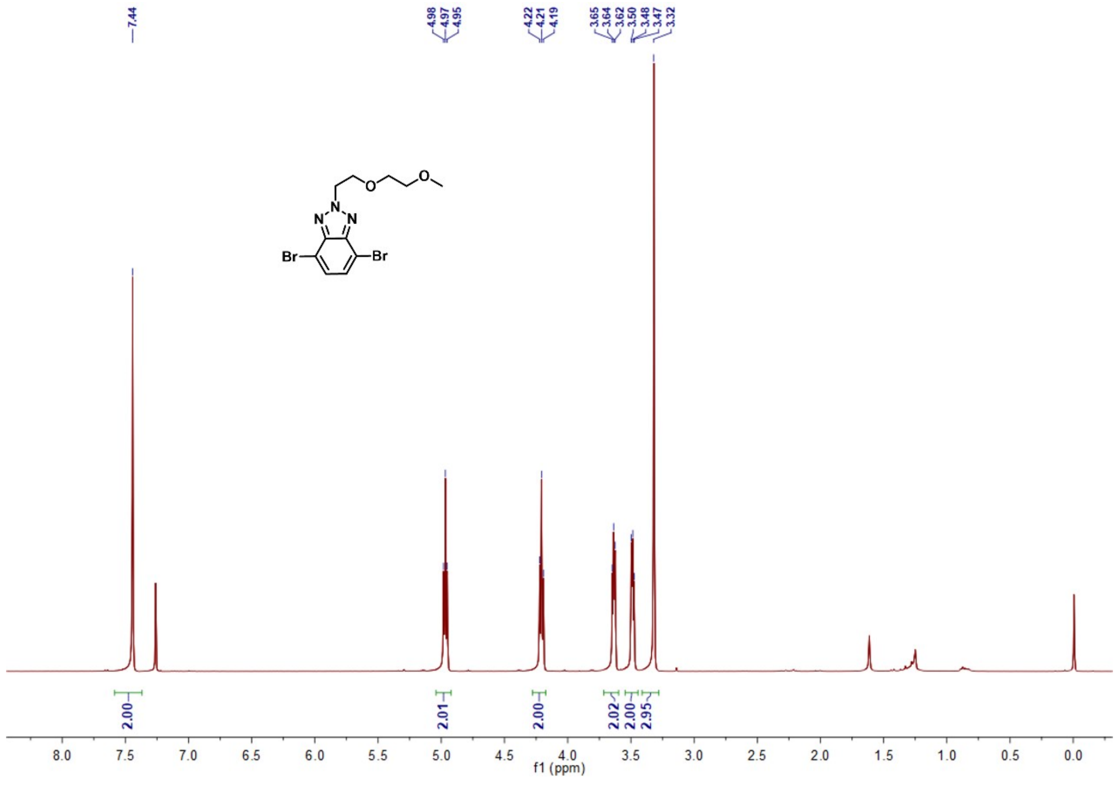

Figure S7 ^{1}H NMR spectrum of 2 in $CDCl_3$.

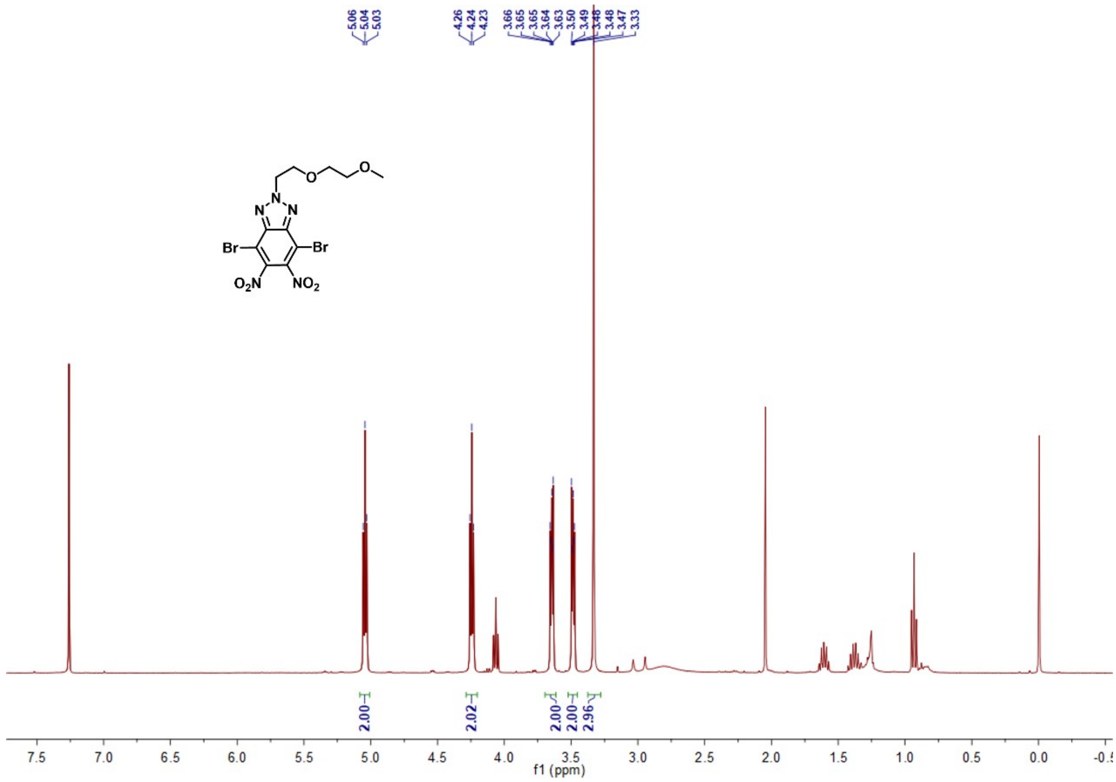

Figure S8 ^{1}H NMR spectrum of 3 in $CDCl_3$.

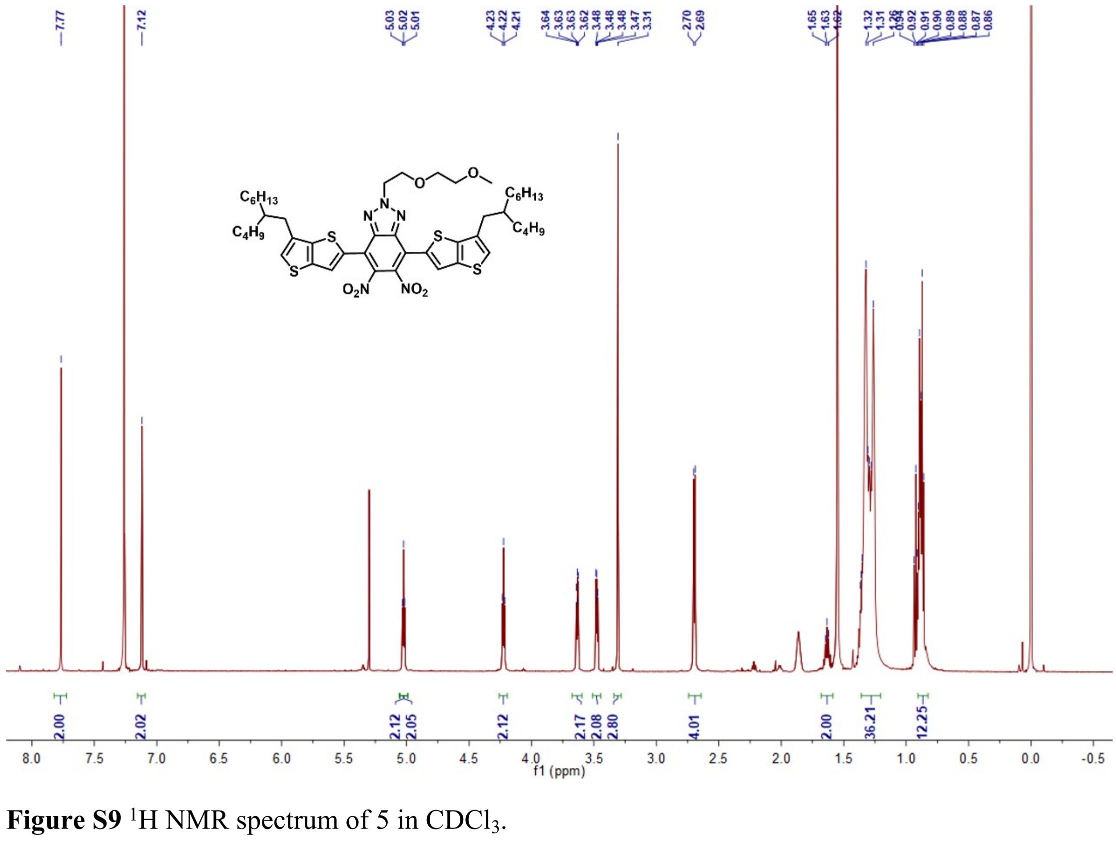

Figure S9 ^{1}H NMR spectrum of 5 in $CDCl_3$.

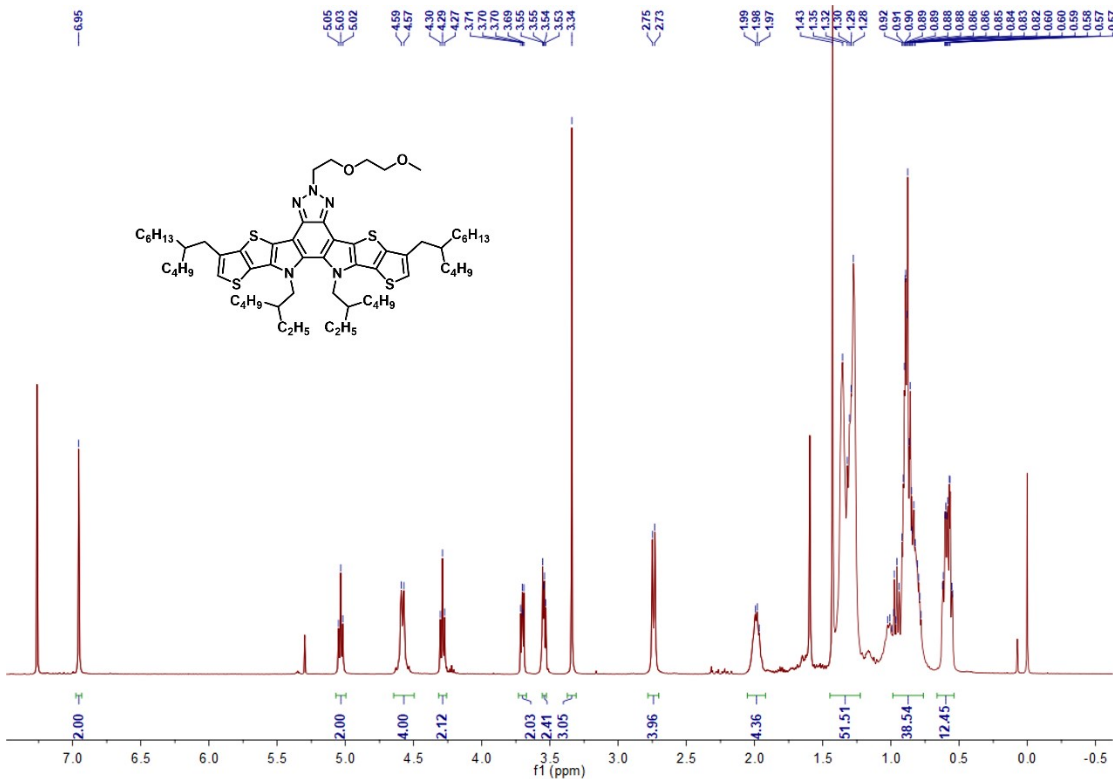

Figure S10 ^{1}H NMR spectrum of 6 in $CDCl_3$.

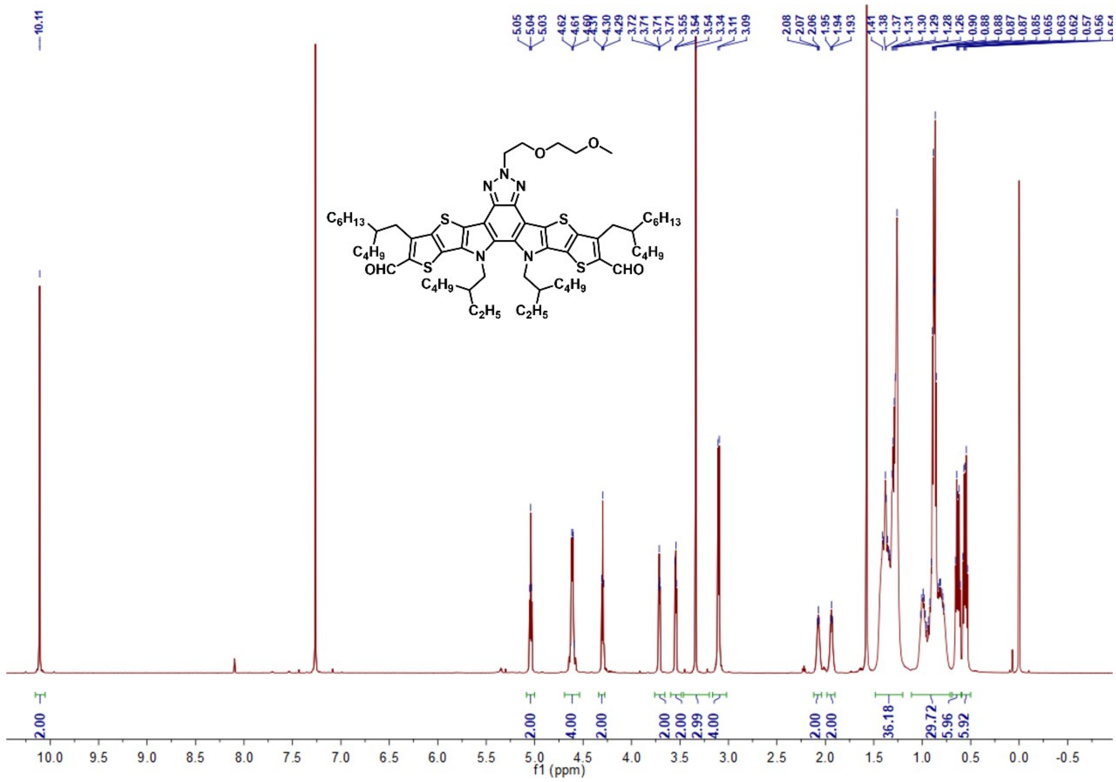

Figure S11 ^{1}H NMR spectrum of 7 in $CDCl_3$.

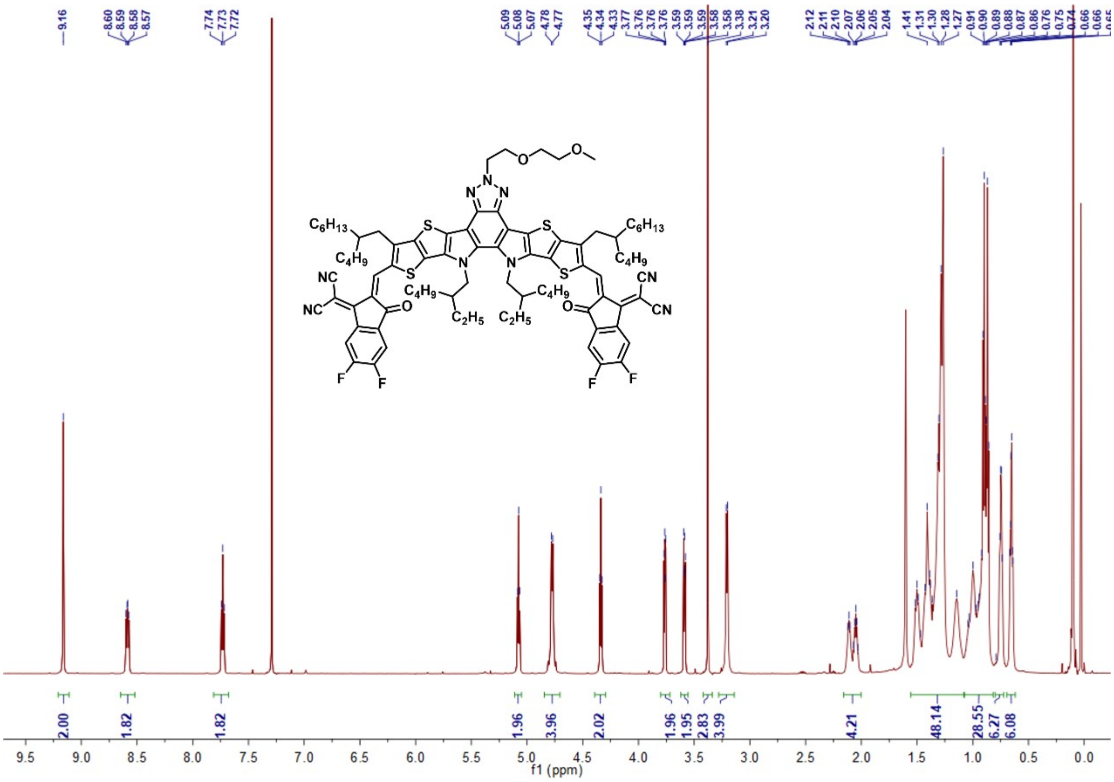

Figure S12 ^{1}H NMR spectrum of L8BO-2O in $CDCl_3$.

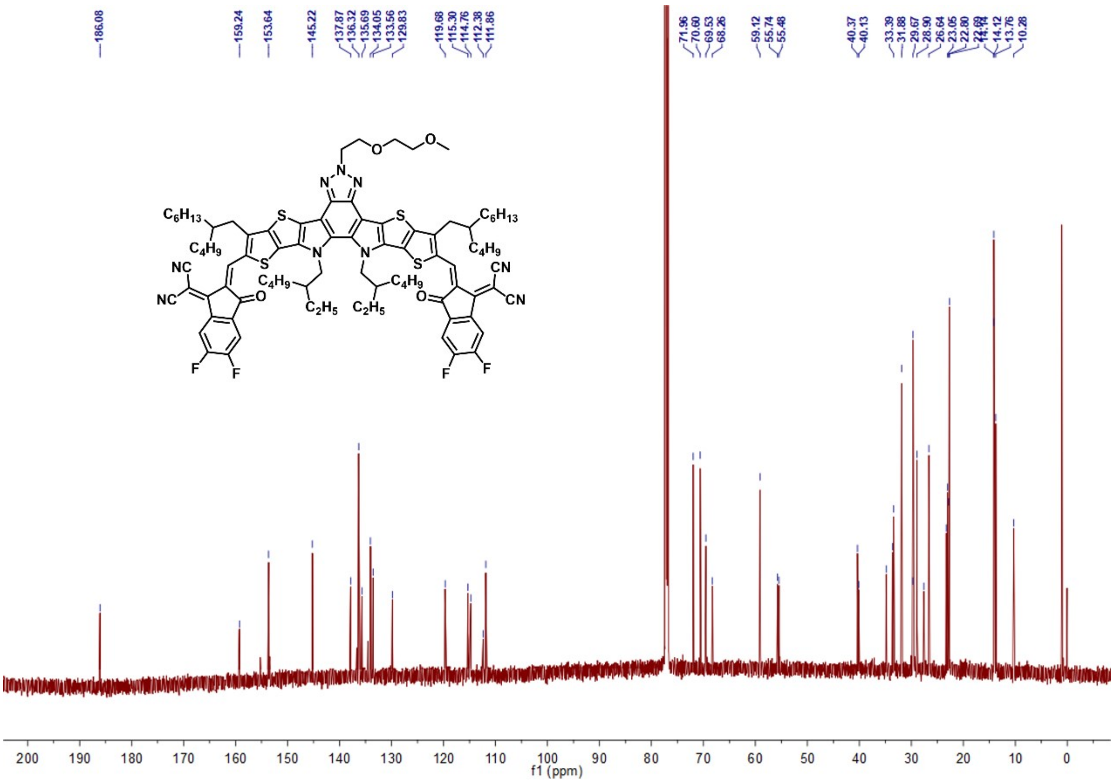

Figure S13 ^{13}C NMR spectrum of L8BO-2O in $CDCl_3$.

2. Materials characterization

Cyclic voltammetry (CV) measurements were performed on a CHI660D electrochemical workstation, equipped with a three-electrode cell consisting of a platinum working electrode, a saturated calomel electrode (SCE) as reference electrode and a platinum wire counter electrode. CV measurements were carried out in anhydrous acetonitrile containing 0.1 Mn-Bu4NPF6 as a supporting electrolyte under an argon atmosphere at a scan rate of 100 mV s^{-1} assuming that the absolute energy level of Fc/Fc^{+} was -4.80 eV. The absorption spectra were recorded using a Hitachi U-4100 UV-Vis scanning spectrophotometer. The contact angles and surface energies were obtained by CSCDIC-200S. The current density-voltage (*J-V*) curves of all the fabricated solar cells were measured under an illumination of AM 1.5G (100 mW cm^{-2}) using a Keithley 2400 and an XES-40S2 (SANEI ELECTRIC Co., Ltd) solar simulator (AAA grade, 70×70 mm^2 photo beam size). The Zolix Solar Cell Scan 100 was used to measure external quantum efficiency (EQE) spectra. The photoluminescence (PL) spectrum, and the atomic force microscopy (AFM) images were measured in the public laboratory of Qingdao Institute of Energy. Grazing incidence wide-angle X-ray scattering (GIWAXS) studies were measured at the synchrotron radiation center of Shanghai light source.

3. Device fabrication

The conventional device structure of ITO/PEDOT: PSS/Active layer/PDINN/Ag is used to construct the devices of the blends. The residual organic matter on the surface of ITO conductive glass was ultrasonically cleaned with a cleaning solution, and then the cleaning solution was removed with deionized water. Next, the ITO conductive glass was ultrasonically cleaned with acetone and isopropyl alcohol in turn, and each step was ultrasonically cleaned for about 20 minutes. After drying, the cleaned ITO conductive glass was treated twice with oxygen plasma for 100 seconds each time before spinning and coating the hole transport (PEDOT: PSS) layer. PEDOT: PSS filtered with 0.45 μm PES is spin-coated on ITO at a rate of 4000 r/min and annealed at 155 °C for 15 min. Transfer the annealed ITO to the glove box with nitrogen atmosphere. In the active layer solution, the donor concentration is fixed as 10.5 mg/ml, and the active layers with different weight ratios (the third component in different proportions of 0 wt%, 20 wt%, 40 wt%, 60 wt%, 80 wt%, 100 wt% is incorporated into the active layer) were dissolved in CB solvent and stirring at 60 °C after 1.5 hours of mixing 0.6% 1-Chlornaphthalene (CN) was added as a liquid additive and mixed for 5 min. The active layer solution is spin-coated at 2700 r/min and annealed at 100 °C for 8 min. The prepared 1 mg/ml PDINN solution (1 mg PDINN and 1 ml methanol were mixed and stirred for 2 hours) was spin-coated onto the active layers at 3000 r/min for 20 s. Finally, in the vacuum condition of 10^{-4} Pa, 80 nm argentum (Ag) was deposited by thermal evaporation with a shadow mask of 0.0936 cm^{-2}.

4. Space charge limited current (SCLC) measurement

The structure of hole-only devices was Glass/ITO/PEDOT: PSS/Active layer/MoO3/Ag (100 nm). The structure of electron-only devices was Glass/ITO/ZnO/Active layer/PDINO/Al (100 nm). The electron and hole mobilities were calculated by using the modified Mott–Gurney equation:

$$J = \frac{8}{9}\varepsilon_0 \varepsilon_r r \mu \frac{V^2}{d^3}$$

where J is the current density, μ is the charge carrier mobility, ε_0 is the permittivity of free space, ε_r is the relative permittivity of the material, d is the thickness of the active layers, and V is the effective voltage. The effective voltage was obtained by subtracting the built-in voltage (V_{bi}) and the voltage drop (Vs) from the series resistance of the whole device except for the active layers from the applied voltage (V_{appl}), $V = V_{appl} - V_{bi} - V_s$. The mobility is calculated from the slope of the J1/2 -V curves.

5. Supplementary Figures and Tables

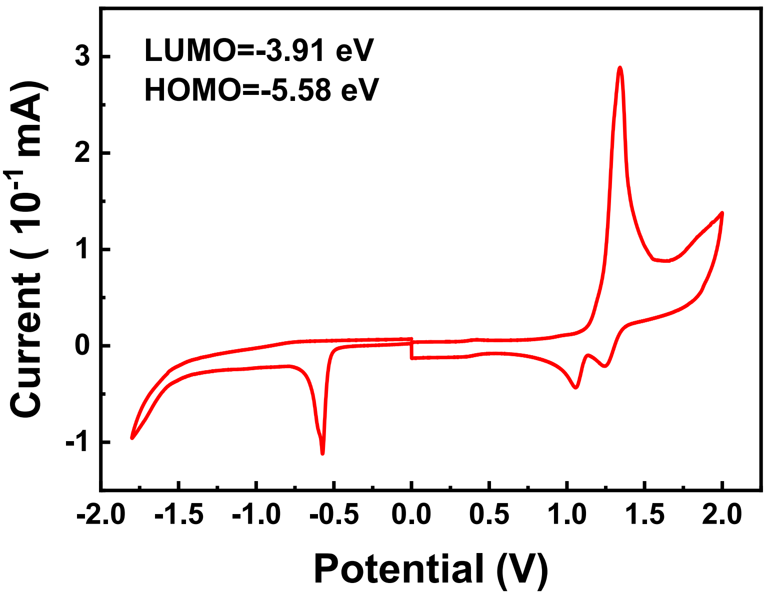

Figure S14 Cyclic-Voltammetry curve of L8BO-2O.

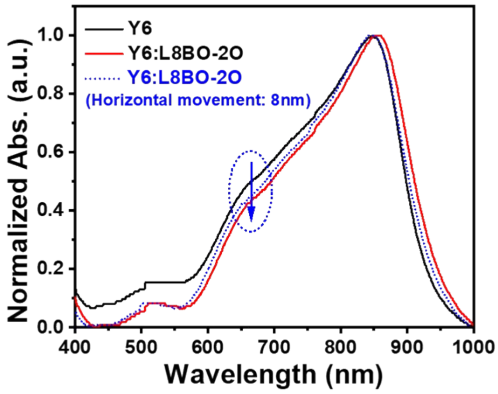

Figure S15 The absorption spectra of Y6 and the Y6:L8BO-2O films.

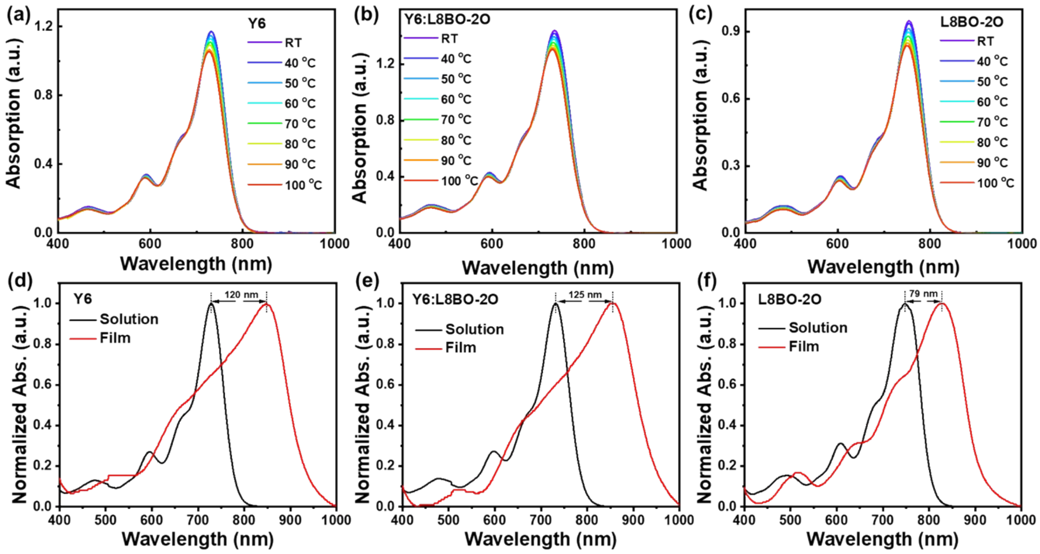

Figure S16 (a-c) The absorption spectra of Y6, L8BO-2O, and the Y6:L8BO-2O mixed acceptor (20% L8BO-2O in Y6) solutions; (d-f) The absorption spectra of Y6, L8BO-2O, and the Y6:L8BO-2O solutions and films.

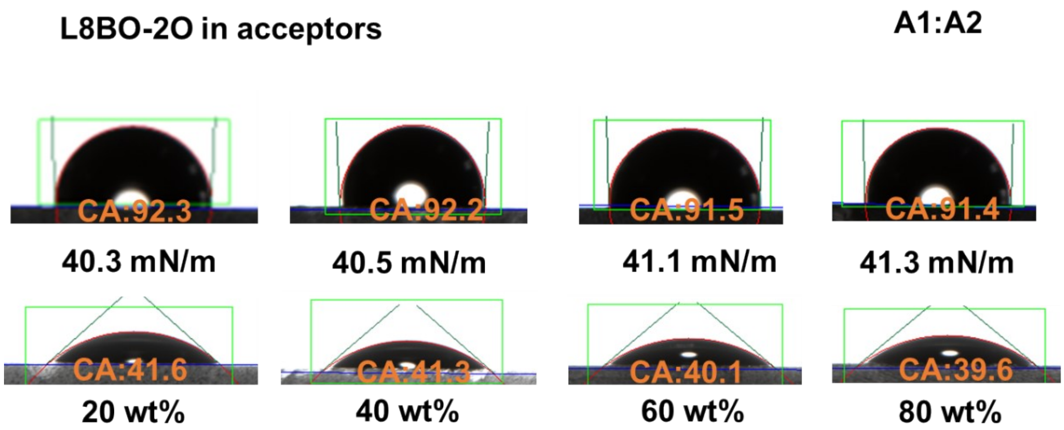

Figure S17 Contact angles of water (top panel) and diiodomethane (bottom panel) droplets on

L8BO-2O:Y6 blend films with different L8BO-2O contents.

Table S1 Photovoltaic parameters of PM6:Y6 based OSCs in high boiling solvent.

Active layer	Solvent	V_{OC} (V)	J_{SC} (mA cm^{-2})	FF (%)	PCE (%)	ref.
PM6:Y6	CB	0.812	24.13	71.36	13.98	*Nat. Energy.*, 2021, **6**,1045-1053
	OXY	0.79	18.41	60.68	8.85	*ACS Appl. Mater. Interfaces.*, 2021, **13**, 59043–59050
	CB	0.78	22.17	68	12.07	*Adv. Funct. Mater.*, 2022, **32**, 2110209
	PX	0.8	22.75	61.81	11.25	*Chin. J. Chem.*, 2022, **40**, 2963-2972
	CB	0.832	24.19	72.4	14.58	*Energy Environ. Mater*., 2022, **5**, 977-985
	OXY	0.82	21.4	63	11.05	*ACS Appl. Mater. Interfaces*., 2023, **15**, 24670–24680
	OXY	0.764	23.88	69.95	12.76	*J. Mater. Chem. C*., 2023, **11**, 13263-13273
	CB	0.799	22.4	70	12.5	*Sol. RRL.*, 2023, **7**, 2201012
	OXY	0.789	19.62	66.3	10.25	*J. Mater. Chem. C*., 2023, **11**, 539-545
	CB	0.789	24.43	69.36	13.37	*Adv. Mater.*, 2023, **35**, 2302946
PM6:Y6	CB	0.82	23.66	74.71	14.54	This work
PM6:Y6:L8BO-2O	CB	0.85	25.22	76.67	16.43	This work

Table S2 The surface energy (γ_s) and Flory-Huggins interaction parameter (χ) for PM6, Y6, and L8BO-2O films.

Film	γ_s (mN m^{-1})	χ (k)
PM6	32.861	0.505 (PM6:L8BO-2O)
Y6	40.573	0.406 (PM6:Y6)
L8BO-2O	41.510	0.005 (Y6:L8BO-2O)

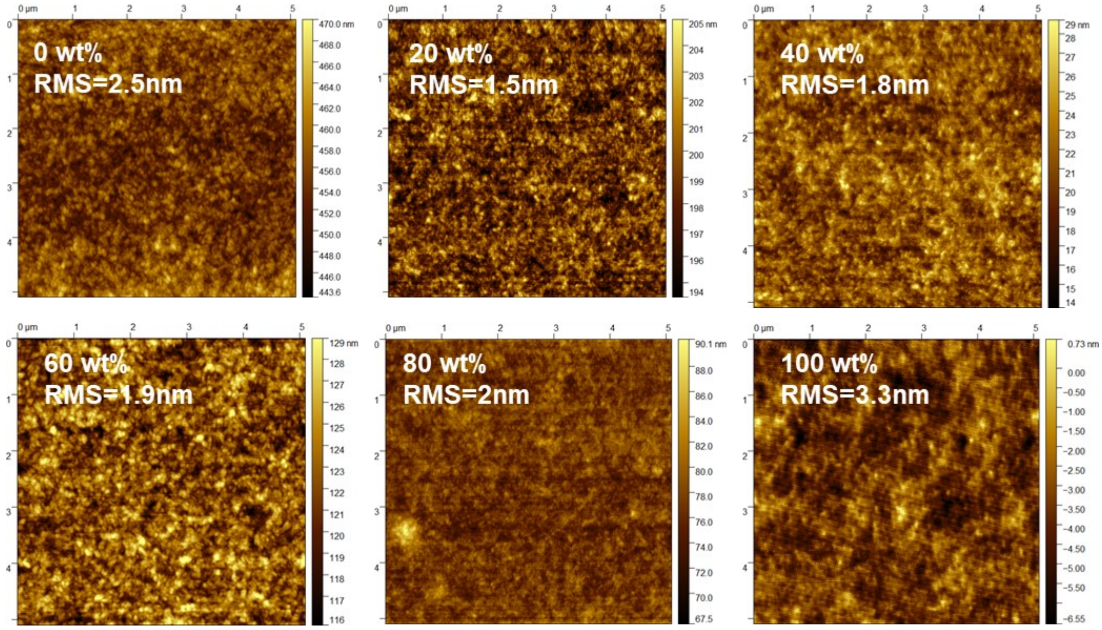

Figure S18 The AFM images of the binary and ternary blend films.

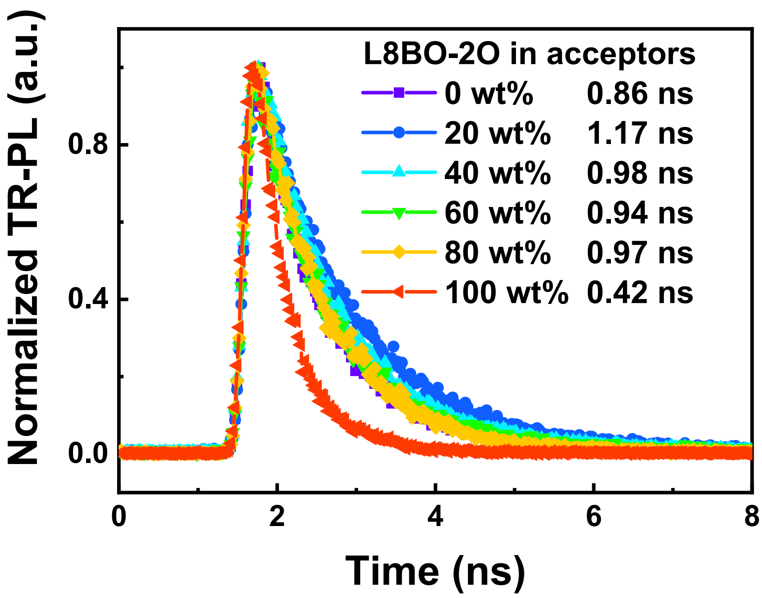

Figure S19 TR-PL Y6 film with different L8BO-2O contents.

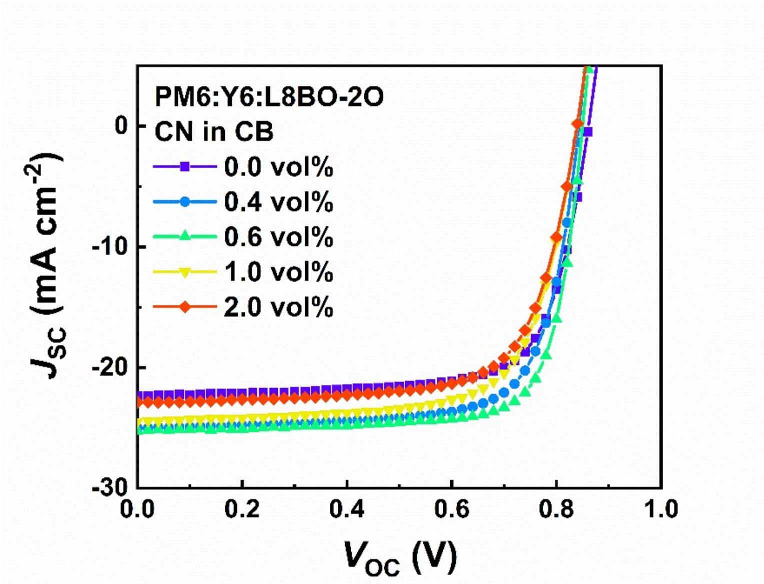

Figure S20 the J-V curves of the optimization process of OSCs.

Table S3 Photovoltaic parameters of the optimization process of OSCs.

Sample	**CN content (vol%)**	**V_{OC} (V)**	**J_{SC} (mA cm^{-2})**	**FF (%)**	**PCE (%)**
	0.0%	0.86	22.33	72.79	14.00
	0.4%	0.84	25.02	73.26	15.46
PM6:L8BO-2O:Y6	0.6%	0.85	25.22	76.67	16.43
	1.0%	0.84	24.42	70.25	14.40
	2.0%	0.84	22.91	70.43	13.54

Table S4 The parameters of exciton dissociation and collection for PM6:Y6 based OSCs with different L8BO-2O contents.

L8BO-2O in acceptors	J_{ph} (mA cm^{-2})	J_{max} (mA cm^{-2})	J_{sat} (mA cm^{-2})	η_{diss} (%)	η_{coll} (%)
0 wt%	22.80	20.02	23.01	0.991	0.870
20 wt%	23.82	21.34	23.99	0.993	0.890
40 wt%	22.98	20.63	23.15	0.993	0.891
60 wt%	22.37	19.68	22.61	0.990	0.870
80 wt%	22.30	19.27	22.60	0.987	0.853
100 wt%	19.22	17.27	19.56	0.983	0.883

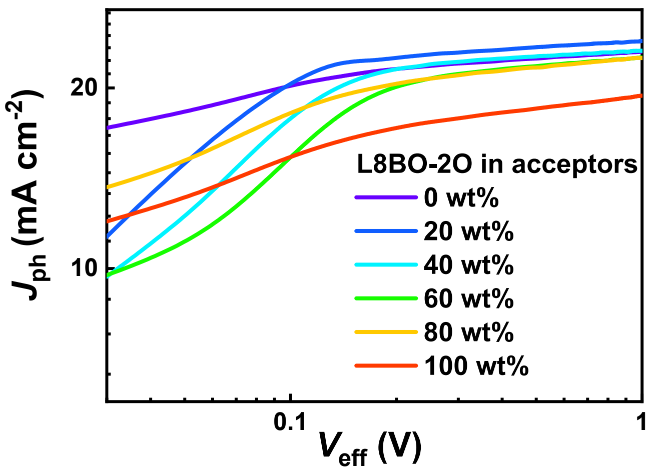

Figure S21 The photocurrent density (J_{ph}) and effective voltage (V_{eff}) curves of binary and ternary OSCs.

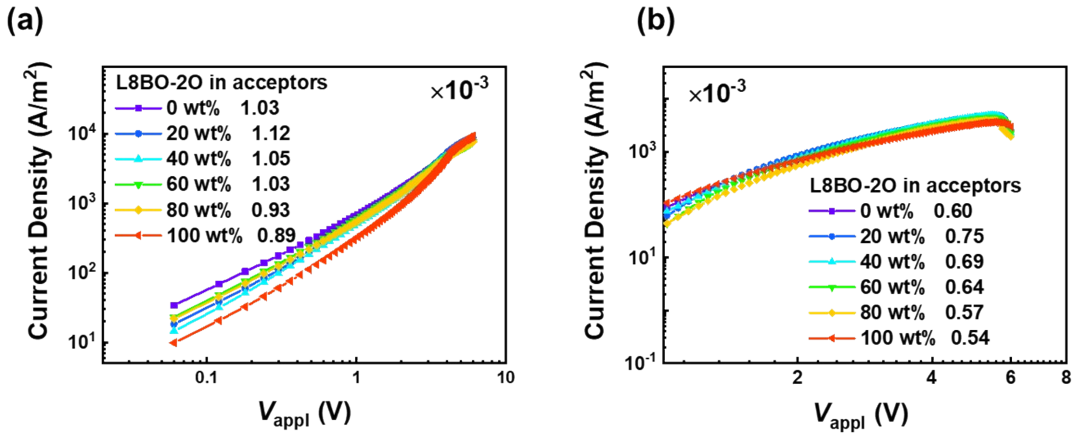

Figure S22 (a) Hole and (b) electron mobility of binary and ternary blend films.

Table S5 The ratios of μ_h/μ_e for binary and ternary blend films.

L8BO-2O in acceptors	μ_h ($\times10^{-3}$ cm^2 V^{-1} S^{-1})	μ_e ($\times10^{-3}$ cm^2 V^{-1} S^{-1})	μ_h/μ_e
0 wt%	1.03	0.60	1.72
20 wt%	1.12	0.75	1.49
40 wt%	1.05	0.69	1.52
60 wt%	1.03	0.64	1.61
80 wt%	0.93	0.57	1.64
100 wt%	0.89	0.55	1.64

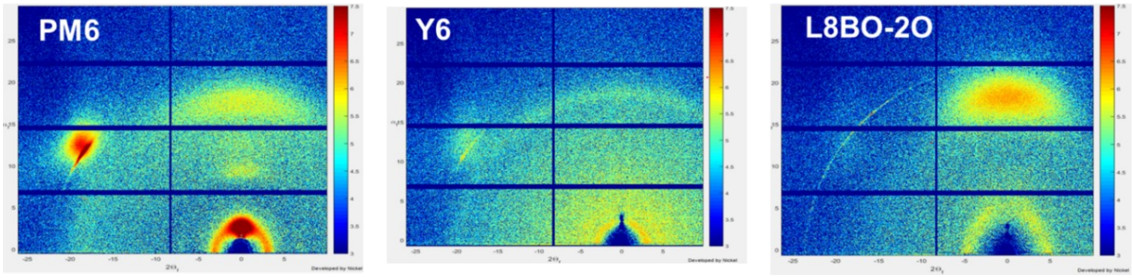

Figure S23 2D-GIWAXS patterns of PM6, Y6 and L8BO-2O neat films.

Table S6 The performance parameters calculated from 2D-GIWAXS test.

L8BO-2O in acceptors	CCL (Å)	π-π stacking distance (Å)
0 wt%	29.09	3.59
20 wt%	31.75	3.60
40 wt%	31.23	3.60
60 wt%	30.39	3.60
100 wt%	28.96	3.59